Title: Effect of Surface Patterning and Presence of Collagen I on the Phenotypic Changes of Embryonic Stem Cell Derived Cardiomyocytes

Authors: Wan, CR[1]; Frohlich EM[3,4].; Charest JL[3]; Kamm RD[1,2]

Departments and Institutions:

Department of Mechanical Engineering[1] and Biological Engineering[2] Massachusetts Institute of Technology, Cambridge, MA, USA;

Charles Stark Draper Laboratory[3], Cambridge, MA, USA

Department of Mechanical Engineering[4], Boston University, Boston, MA, USA

Address: 77 Massachusetts Avenue, NE47-313, Cambridge, MA, 02139

Abbreviated title: Surface Patterns and Collagen I Affect Myocyte Phenotype

Corresponding author: Roger D. Kamm, Ph.D;

77 Massachusetts Avenue NE47-321, Cambridge, MA, 02139

Tel: (617) 253-5300

Fax: (617) 258-8559

rdkamm@mit.edu

Abstract

Embryonic stem cell derived cardiomyocytes have been widely investigated for stem cell therapy or *in vitro* model systems. This study examines how two specific biophysical stimuli, collagen I and cell alignment, affect the phenotypes of embryonic stem cell derived cardiomyocytes *in vitro*. Three phenotypic indicators are assessed: sarcomere organization, cell elongation, and percentage of binucleation. Murine embryonic stem cells were differentiated in a hanging drop assay and cardiomyocytes expressing GFP-α-actinin were isolated by fluorescent sorting. First, the effect of collagen I was investigated. Addition of soluble collagen I markedly reduced binucleation as a result of an increase in cytokinesis. Laden with a collagen gel layer, myocyte mobility and cell shape change were impeded. Second, the effect of cell alignment by microcontact printing and nanopattern topography was investigated. Both patterning techniques induced cell alignment and elongation. Microcontact printing of 20μm line pattern accelerated binucleation and nanotopography with 700nm ridges and 3.5μm grooves negatively regulated binucleation. This study highlights the importance of biophysical cues in the morphological changes of differentiated cardiomyocytes and may have important implications on how these cells incorporate into the native myocardium.

Key terms: microcontact printing, nanopattern, hanging drop, embryonic stem cell differentiation, cardiogenesis, extracellular matrix, myocytes, stem cell therapy, binucleation

Introduction

The ability of embryonic stem cells to differentiate into cardiomyocytes *in vitro* has motivated numerous studies of possible clinical application,[24, 32, 48] development of *in vitro* model systems,[4, 21, 40] and/or generation of a continuous source of contractile cells. Some challenges remain, however, such as how to drive embryonic stem cell derived cardiomyocytes (ESCDMs) into maturation.[30, 38, 43] In this study, we attempt to characterize the phenotypic changes of ESCDMs with respect to two biophysical stimuli – presence of collagen I and cell alignment.

Collagen I is a critical ECM component in the adult myocardium and a ubiquitous cardiac tissue engineering scaffold material.[7, 8, 56] The integrin interactions of collagen I in cardiac tissue have also been well studied.[9, 16, 29] For highly contractile cells, an overlay of collagen I scaffold has been demonstrated to enhance differentiation and increase contractile protein production *in vitro*.[49] Some preliminary evidence suggests that by injecting collagen I hydrogel with neonatal myocytes into infarcted tissue, cardiac ejection fraction is improved.[27] However, more mechanistic studies are required to understand how ECM proteins, collagen I in particular, impact ESCDM function.[4, 27, 57]

The second biophysical stimulation we focused on is cell alignment. In the myocardium, cardiomyocytes are arranged into layered two-dimensional sheets, precisely oriented to produce a twisting motion during each contraction.[1, 31] Two ways to induce alignment have been explored *in vitro* – protein patterning, also known as microcontact printing, and topographical patterning. Both patterning techniques can induce anisotropy of neonatal myocyte monolayers.[2, 17, 23, 25] However, the mechanisms by which patterns affect ESCDM phenotype remains elusive.

In this study, we investigated how two specific biophysical stimuli, collagen I and cell alignment, affect the morphology of embryonic stem cell derived cardiomyocytes. Three phenotypic indicators commonly used to characterize a more mature morphology were used – sarcomere organization, cell elongation, and

binucleation.[39, 43, 44, 50] While surface patterning and ECM interactions have been studied extensively for neonatal myocytes *in vitro*, the effects are lesser known for ESCDMs.[3, 17, 19, 42] Based on this previous work, we hypothesized that both cell alignment and interactions with collagen I would enhance the rate of differentiation of ESCDMs. This study is an important step toward an improved understanding of how the biophysical environment affects ESCDMs.

Materials and Methods

Cell Culture and Differentiation

Murine embryonic stem cells (mESC - line CGR8) were kindly provided by Dr. Richard Lee, Harvard Medical School. The cardiac specific α-MHC promoter was tagged with green fluorescent protein (GFP) and thus differentiation could be readily assessed via observation of GFP. To keep ESCs undifferentiated, leukemia inhibitory factor (LIF) was present in the medium, comprised of Glasgow Minimum Essential Medium (GMEM) (Invitrogen), 1,000U/ml Leukemia Inhibitory Factor (Sigma), 1mM Sodium Pyruvate (Invitrogen), 1x Non-Essential Amino Acid (Invitrogen), 15% Knockout Serum Replacement (Invitrogen), 25mM of HEPES, 10^{-4}M β- mercaptoethanol (Sigma), and 1x Penicillin-Streptomycin (Invitrogen). Cells were maintained in flasks coated with 0.1% gelatin in PBS. Cell confluency was tightly controlled not to exceed 70%.

By removing LIF and creating a three-dimensional environment, mESCs spontaneously differentiate. The composition of the differentiation medium was similar to that of the maintaining medium. In addition to the removal of LIF, knockout serum replacement was replaced by ESC Fetal Bovine Serum (Invitrogen). 100μM of ascorbic acid was added to enhance differentiation.[46]

A standard hanging drop technique was used to induce differentiation.[37] Briefly, cell suspension solution was prepared at 10,000 cells/ml. 30μl drops were placed on the inside of a 100mm non-tissue culture treated Petri dish, containing 10ml of 1x PBS. Drops, containing small cell aggregates, were cultured for

2 days before being collected with a 10ml pipette. These aggregates continued to be cultured, in differentiation medium, for 3 more days for embryoid body (EB) formation. Once EBs were formed, they were collected, seeded on 0.1% gelatin coated 6-well plates and cultured for 4 more days before being dissociated and isolated with fluorescent-based sorting. Upon plating, spontaneous contraction and GFP expression could be observed usually within 72-96 hours.

Isolation and Cell Seeding

EBs are composed of stem cells with extensive extracellular matrix proteins and thus standard trypsinization alone was not sufficient. Instead, EBs were first washed with PBS twice and incubated with 0.05% trypsin for 5-7 minutes. After that, EBs were dislodged from the culturing substrate with gentle agitation using a 1ml pipettor and transferred into a test tube where ample media were added to neutralize the effect of trypsin. At this point, many clumps were still present and the test tube was centrifuged for 5 minutes at 1,200rpm. After the removal of the supernatant, more trypsin was added and the cells incubated for another 5-7 minutes. This second stage caused most of the cells to dissociate. Medium was added and the solution was centrifuged again. Once all trypsin-containing media were replaced by fresh media, the content was passed through a 40μm cell strainer and transferred to a test tube for sorting. Fluorescent activated cell sorting was performed with MoFlo (Cytomation). Either differentiated ESCs without GFP or undifferentiated ESCs were used as the negative control. 2-4% of total cells were GFP-positive and the purity of the sorted population was consistently higher than 99.95%.

The purified population of cells was resuspended in warm medium to a concentration of 2,000,000 cells/ml. Four collagen conditions were examined: ESCDM monolayer with no collagen (control), ESCDM monolayer supplemented with 50μg/ml of soluble collagen I, ESCDM monolayer laden with 2mg/ml collagen I hydrogel and isolated ESCDMs suspended in 2mg/ml collagen I hydrogel. ESCDM monolayer seeding density was 100,000 cells/cm^2, due to the limited ability for differentiated cardiomyocytes to divide and proliferate. In the soluble collagen condition, the small amount of collagen

did not affect the pH of the medium. In the condition with a collagen gel overlay, 2mg/ml collagen gel, prepared on ice, was reconstituted by combining 10x DMEM, 0.5N NaOH, high concentration (3-4 mg/ml) collagen I (BD Biosciences) and sterile cell culture grade water. 30µl of gel solution was used for each 96 well plate, resulting in a hydrogel layer several hundred microns thick. The gel was polymerized for 40 minutes in the incubator (37°C, 5% CO_2), followed by the addition of warm medium. The scaffold was added to the cell monolayer three days after seeding, when most cells had fully spread and formed confluent monolayers. For the condition with ESCDMs suspended in collagen gel, the same collagen recipe was followed except that water was replaced with cell solution for a final concentration of $1.5x10^6$ or $5x10^6$ cells/ml.

Microcontact Printing

Microcontact printing is a technique to transfer specific proteins between two solid surfaces. The procedure used is similar to that described in Feinberg et. al..[17] Briefly, molds were fabricated by standard soft lithography and stamps with a 20µm/20µm line pattern were made with polydimethylsiloxane (PDMS). Stamps were sterilized by sonication in 50% ethanol for 30 minutes and stored in 70% ethanol. Stamps were washed, dried and incubated with 0.1% Oregon-green conjugated gelatin (Invitrogen) for 1 hour. Rinsed and dried stamps were lowered onto plasma treated surface to initiate contact and pressed for 1 minute with mild pressure allowing for proper protein transfer.

In the following steps, one rinse with sterile PBS was performed between each step. 1% Pluronics-F127 (Sigma) was added to the stamped and rinsed surface for 15 minutes, followed by incubation of 0.02% nonfluorescent gelatin (Gibco) for 15 minutes. Finally, the surfaces were rinsed three times before being stored in PBS in the incubator.

Nanopattern Topography

Hot embossing generated the submicron-scale substrate topography with an epoxy mold created by a three-step molding process. First, a silicon master mold was fabricated using standard photolithography

and reactive ion etching (RIE). A 1 μm-thick layer of silicon oxide was thermally grown on a 100 mm silicon wafer and features ranging from 500 nm to 1 μm were created by spin-coating a 500 nm layer of Shipley 1805 photoresist on the wafer, patterning the photoresist using a standard photomask, and developing the patterned photoresist. An anisotropic reactive ion etch using CF_4 and O_2 transferred the photoresist features into the silicon oxide to a depth of 1 μm before stripping the photoresist. The second mold was made with PDMS. The third epoxy mold was made from a two-part high temperature epoxy (Conapoxy FR-1080, CYTEC Industries). For the hot embossing step, the epoxy mold was placed with the submicron features in contact with a thermoplastic polystyrene blank in a uniformly heated, temperature- and pressure-controlled press. The resulting substrate was a relief replica of the silicon master mold and served as the platform for cell culture experiments.

Immunofluorescent Labeling

To visualize sarcomere organization, cells were first washed twice with 1x PBS to remove media and fixed with 4% paraformaldehyde (PFA) for 15 minutes in room temperature. 0.1% triton-x was used to permeabilize the cell membrane for 2-5 minutes. For the following steps, 2D cultures were incubated with the appropriate reagent for 1hr at room temperature, and 3D cultures were incubated overnight at 4°C. Cells were first incubated with block ace (Dainippon Pharmaceutical, Tokyo, Japan) to block nonspecific binding, followed by incubation of primary antibodies, mouse sarcomeric α-actinin, at dilution factor of 1:200. Secondary detection antibody (anti-mouse Alexa 568) and 4',6-diamidino-2-phenylindole (DAPI) were used to visualize protein of interest and nuclei respectively. In between each of the steps described previously, two rinses of 1x PBS were performed. For samples with collagen gel, longer washing procedures were adapted and secondary antibody was reconstituted in PBS with 2% rabbit serum and 2% bovine serum albumin to further reduce background staining.

Quantification and Statistical Analysis of Binucleation, Cell Shape and Cell Alignment

Cell elongation, binucleation and cell orientation were quantified by ImageJ. To quantify elongation, individual GFP-positive cells were identified, traced and fitted as ellipses. Then the ratio of major and minor axis, the aspect ratio, was calculated. For each condition, 10-30 separate regions (330μm x 430μm) were imaged and a total of 60-100 randomly selected cells were traced. Thus, the majority of the cells traced were not in contact with each other. To quantify binucleation, each GFP image was merged with DAPI image to enhance the identification of nuclei. Number of binucleated cells were then counted. At least 500 GFP-positive cells were counted for each experimental condition. To measure alignment angle, pattern angle was first determined and then the deviation angle of the major axis of the cell and the pattern angle was calculated. At least three independent sets of experiments were performed for each condition.

Data were expressed as mean ± SEM and analyzed using one-way ANOVA followed by post hoc Student's t test. Results with $P<0.05$ were considered statistically significant.

Results

Sarcomere development of ESCDMs suspended in collagen gel or plated on ECM-coated polystyrene

In this study, we were interested in how biophysical stimulations affect the morphology of ESCDMs. We started the investigation with collagen I, a ubiquitous ECM protein in the adult heart as well as in previous *in vitro* cell culture with cardiomyocytes.[21, 56] We found that suspending ESCDMs in 2mg/ml collagen gel does not induce sarcomere development or cell-cell contacts, two key parameters observed during proper cardiomyocyte development (Figure 1).[13, 28, 41] Isolated ESCDMs remain rounded and contractile. Immunofluorescent staining of sarcomeric α-actinin reveals a punctate protein distribution, lacking any organized structures. Two cell seeding densities ($1.5x10^6$ and $5x10^6$ cells/ml) exhibited similar results. These findings suggest that static culture of single ESCDMs suspended in collagen I gel is not conducive for myocyte development.

In contrast, confluent ESCDM monolayers with well-developed sarcomeres, along with stress fibers, are observed in cells seeded on ECM-coated polystyrene. Sarcomeres, albeit immature, can be observed 48 hours after seeding and become more clearly evident for all three conditions – no collagen, with soluble collagen and with a laden layer of collagen gel (Figure 2a).

Effect of collagen I on cell elongation

Elongation of ESCDMs was measured by the aspect ratio – the ratio of the major and minor axis -- of each cell. Figure 2b shows the aspect ratio of ESCDMs over time, exposed to collagen I in different forms. Regardless of how collagen I is presented to the cell monolayer, cell aspect ratio increases over time. The aspect ratio of ESCDMs laden with a layer of collagen I is reduced slightly but significantly compared to control where no additional collagen is added. Interestingly, the rate of increase in aspect ratio is dependent upon the collagen condition (Figure 2c). Clear increase in aspect ratio over time can be observed for the three different collagen I conditions but the increase of aspect ratio is highest for the soluble collagen condition, followed by the control condition and the collagen gel condition. On average, the aspect ratio of ESCDMs increases by 9.6% per day for the condition with soluble collagen, 7.5% for control, and 4.6% for the condition with collagen gel.

Effect of collagen I on cell binucleation

Binucleation, like cell elongation measured by aspect ratio, increases over time (Figure 3a). Binucleation has been suggested to be a phenotypic indicator of maturation *in vivo* and *in vitro*.[44, 53] Effects of collagen I on binucleation depend on how collagen I is presented. Presented as a hydrogel, it has little impact on binucleation. A small increase in binucleation can be seen after 2 weeks of culture with collagen gel, compared with control. When collagen I solution is added into the medium, it strongly inhibits binucleation. After 14 days, ESCDMs cultured with soluble collagen have 50% fewer binucleated cells compared with the control.

To confirm whether the reduction of binucleation is due to a decrease in karyokinesis or an increase of cytokinesis, we counted the number of cells. We found an increasing number of cells when ESCDMs are cultured with soluble collagen I, under which condition ESCDMs are more likely to undergo cytokinesis and complete the cell cycle (Figure 3b).

Effect of Surface Patterning on ESCDM Alignment

The second biophysical cue we investigated is cell alignment. ESCDMs cultured on MCP and NPT surfaces align with the pattern surface (Figure 4). For the MCP surface, gelatin conjugated with Oregon Green is used to visualize and measure the pattern angle. For the NPT surface, the ridges and grooves alter between 3.5μm and 700nm. Aligned sarcomeres can be observed for both patterning techniques. Sarcomere development is strongly dependent on the periodicity of NPT surface as the sarcomere width coincides with the width of the ridges. This same phenomenon is not observed for MCP surface.

For cells cultured on MCP and NPT surfaces, the angle between the major axis of the cell and the pattern was calculated (Figure 5). Alignment can be observed within 48 hours: almost all cells cultured on MCP and NPT surfaces align within 20 degrees of the pattern orientation (Figure 5a). The same strong alignments persist over time (Figure 5b&c). By day 7, more than 70% of the cells cultured on NPT surfaces align within 10 degrees from the pattern. Interestingly, cell alignment on MCP surface is better retained with collagen gel overlay after 2 weeks. 60% of cells in that condition remained aligned within 10 degrees while alignment in other conditions declined to 30% (Figure 5d).

Effect of Surface Patterning on ESCDM Elongation

Cells cultured on patterned surfaces, both MCP and NPT, exhibit elongated features (Figure 4) although the rate of elongation is highest for cells cultured on isotropic surfaces (Figure 6a&b). There is virtually no increase in aspect ratio for cells on MCP surfaces suggesting that the cellular response to the surface has saturated after 48 hours.

Elongation is mostly attributed to a decrease in minor axis length rather than an increase in major axis length (Figure 6 c&d). Significant reductions in minor axis are observed for both the isotropic and NPT conditions and this explains the shrinkage of the monolayer away from the walls at longer time points.

Effects of surface patterning on binucleation

Percentage of binucleation increases over time for all patterning conditions. Binucleation rate between day 2 and day 7 of ESCDMs on MCP surface is much higher than in cells on isotropic surfaces (Figure 7a). Markedly reduced binucleation was observed for ESCDMs on NPT surfaces, compared with isotropic surface regardless of presence of collagen gel (Figure 7b). We found an increase in the number of ESCDMs on NPT surfaces indicating that the reduction in binucleated cells is a result of cells completing the cell cycle and being able to undergo cytokinesis (Figure 7c). This is similar to the finding for ESCDMs cultured with soluble collagen.

Discussion

In this study, we explored the effects of cell alignment and the addition of extracellular matrix protein, collagen I specifically, on changes of embryonic stem cell derived cardiomyocytes phenotype. This work is motivated by two observations. First, due to the limited regenerative ability of the heart,[55] differentiated stem cells have been considered as a possible source of functional cardiomyocytes. They can also be used as *in vitro* model systems.[11, 35] Second, spontaneously contractile cardiomyocytes can be used as miniature actuators. To date, most research focused on biomachines utilizes neonatal myocytes.[26, 47, 51] Stem cell derived cardiomyocytes have the advantage of being an unlimited and continuous source of contractile cells. However, little is known about how biophysical factors affect ESCDMs and we attempt here to gain a better understanding by first probing two stimuli inspired by the natural environment of the myocardium as well as the previous literature.

We have portrayed a rather complex picture of the relationship between collagen I and ESCDMs. We chose collagen I because of its abundance in the adult heart even though other ECM proteins are present at various stages during development.[7] It is also ubiquitously used as a tissue engineering scaffold *in vitro*.[33, 49] First, we observed that by suspending ESCDMs in collagen as single cells statically, no sarcomeres or cell-cell contacts are formed, even at a high cell density. This result is similar to the findings from Souren et. al. where neonatal cardiomyocytes embedded in collagen gel remain isolated and contract asynchronously.[45] The lack of adequate growth factors or matrix proteins may be one explanation for this finding since Zimmermann et. al. successfully developed 3D cardiomyocyte construct with the addition of Matrigel™ and chick serum.[56] Another possible explanation is that the stiffness of the hydrogel, estimated around 10 KPa,[52] is softer than optimal for myogenesis.[5, 15, 22] On the other hand, according to Discher et. al., substrates that are too stiff, such as polystyrene, are suboptimal for myocyte development as well.[14] However the stiffer substrate is better able to withstand the traction force required for sarcomere development,[42, 54] and this may provide another possible explanation for the differences observed.

Secondly, cell elongation is impeded and alignment maintained in the presence of collagen gel overlay. (Figure 2b) This might be due to the physical constraint the hydrogel imposes on the monolayer, perhaps by binding to the monolayer, and/or by the weight of the gel. One study has found that a collagen gel overlay improved the differentiation of skeletal myotubes presumably by imposing a constant load on the monolayer.[49] Combined with MCP, the collagen gel accelerates binucleation, as demonstrated by the significant increase in binucleation between days 2 and 7, although the increase in binucleation between day 7 and 14 is not statistically different from control (Figure 7a). Although the mechanism of this phenomenon remains to be elucidated, this finding is one example of the combinatorial effects of two biophysical stimulations on ESCDMs.

While this study focuses on the effects of collagen I, other ECM proteins, such as vitronectin or fibronection, may be present in the experimental system due to the presence of serum in the medium. These ECM-integrin interactions have been demonstrated to be critical during heart development.[8, 20, 36] In this study, variation due to the presence of serum was mitigated by using the same lot of serum although further studies could be envisioned to specifically investigate the effects of other ECM proteins on ESCDMs.

Lastly and unexpectedly, collagen I, presented in a soluble form in medium, is a strong negative regulator of binucleation. This effect is not seen when it is presented as a hydrogel. Soluble collagen increases cytokinesis and promotes ESCDMs to complete the cell cycle. This suggests that how ESCDMs respond to collagen I depends on the way it is presented to the cells. This is reminiscent to the differential responses of cells to exogenous and matrix-bound growth factors and this finding is, to our understanding, the first study to explore the effects of exogenous collagen I on ESCDMs.[12]

The second biophysical stimulation we tested is the effect of cell alignment, induced by microcontact printing and nanopattern topography, on ESCDM morphology. In this study, only one set of geometric dimensions of each patterning techniques is explored. Bursac et. al. found that varying MCP dimensions did not cause a statistically significant difference in the electrophysiological properties of neonatal myocytes.[10] For nanoscale topography, Au et. al. found neonatal myocytes exhibited clearer sarcomere structures on surfaces with 0.5μm-wide ridges and 0.5μm-wide grooves than 1μm-wide ridges and 3μm-wide grooves, although it is unclear whether the difference arises from differences in duty cycle or the exact dimensions.[2] Due to the limited understanding of the effects of NPT and the difficulty to directly compare the two patterning techniques, [2, 25] we focused on characterizing their effects on ESCDMs separately compared with the isotropic control.

In this study, consistent with previous literature, we report that both patterning techniques induce cell alignment and elongation, as observed in cardiomyocyte sheets *in vivo*.[7] The increase in aspect ratio over

time is mostly attributed to a decrease in width and the lateral dimensions of the cells remain significantly smaller than adult myocytes (although cell volumes were not measured).[6] Longer culture times and mechanical/electrical stimulations may be necessary for enhanced differentiation and maturation.[18, 34, 43]

In terms of binucleation, the MCP surface alone, without the addition of collagen, slightly but significantly increased the percentage of binucleation compared with a smooth surface. In contrast, compared with the isotropic case, ESCDMs cultured on NPT surface observed markedly reduced binucleation, due to increased cytokinesis. It is reasonable to believe that the finding for MCP surfaces is less dependent on the geometric dimensions but it is less clear whether varying NPT dimensions will produce the same finding. Nevertheless, from this study, we are able to conclude that induced cell alignment affects the binucleation of ESCDMs *in vitro*.

Presence of collagen I and alignment are two important biophysical characteristics of the adult myocardium and here we adopted these two stimuli and characterized their effects on ESCDM phenotypic changes *in vitro*. We are able to demonstrate that by affecting them, we can alter the morphology of embryonic stem cell derived cardiomyocytes. This is an important step in advancing our understanding of how to utilize embryonic stem cell derived cardiomyocytes as a cardiovascular disease treatment option. By being able to control the phenotype *in vitro*, this opens the prospect of using ESCDMs as actuators for biomachines.

Acknowledgements

The authors would like to acknowledge the contribution of Dr. Richard Lee for his invaluable suggestions for this work. We acknowledge the funding support from Singapore-MIT Alliance for Research and Technology to Roger D. Kamm, the Charles Stark Draper Laboratory Internal Research and Development Program to Joseph Charest and Else Frohlich, and American Heart Association Predoctoral Fellowship to Chen-rei Wan.

References

1. Arts, T., K. D. Costa, J. W. Covell, and A. D. McCulloch. Relating myocardial laminar architecture to shear strain and muscle fiber orientation. Am. J. Physiol. -Heart Circul. Physiol. 280:H2222-H2229, 2001.

2. Au, H. T. H., B. Cui, Z. E. Chu, T. Veres, and M. Radisic. Cell culture chips for simultaneous application of topographical and electrical cues enhance phenotype of cardiomyocytes. Lab Chip 9:564-575, 2009.

3. Baharvand, H., M. Azarnia, K. Parivar, and S. K. Ashtiani. The effect of extracellular matrix on embryonic stem cell-derived cardiomyocytes. J. Mol. Cell. Cardiol. 38:495-503, 2005.

4. Baharvand, H., A. Piryaei, R. Rohani, A. Taei, M. H. Heidari, and A. Hosseini. Ultrastructural comparison of developing mouse embryonic stem cell- and in vivo-derived cardiomyocytes. Cell Biol. Int. 30:800-807, 2006.

5. Bhana, B., R. K. Iyer, W. L. Chen, R. Zhao, K. L. Sider, M. Likhitpanichkul, C. A. Simmons, and M. Radisic. Influence of substrate stiffness on the phenotype of heart cells Biotechnol. Bioeng. 105:1148-1160, 2010.

6. Bird, S. D., P. A. Doevendans, M. A. van Rooijen, A. B. de la Riviere, R. J. Hassink, R. Passier, and C. L. Mummery. The human adult cardiomyocyte phenotype. Cardiovasc. Res. 58:423-434, 2003.

7. Borg, T. K. and J. B. Caulfield. The collagen matrix of the heart Fed. Proc. 40:2037-2041, 1981.

8. Borg, T. K., K. Rubin, E. Lundgren, K. Borg, and B. Obrink. Recognition of extracellular matrix components by neonatal and adult cardiac myocytes Dev. Biol. 104:86-96, 1984.

9. Bullard, T. A., T. K. Borg, and R. L. Price. The expression and role of protein kinase C in neonatal cardiac myocyte attachment, cell volume, and myofibril formation is dependent on the composition of the extracellular matrix. Microsc. Microanal. 11:224-234, 2005.

10. Bursac, N., K. K. Parker, S. Iravanian, and L. Tung. Cardiomyocyte cultures with controlled macroscopic anisotropy: a model for functional electrophysiological studies of cardiac muscle Circ. Res. 91:e45-54, 2002.

11. Caspi, O., I. Itzhaki, I. Kehat, A. Gepstein, G. Arbel, I. Huber, J. Satin, and L. Gepstein. In vitro electrophysiological drug testing using human embryonic stem cell derived cardiomyocytes Stem Cells Dev. 18:161-172, 2009.

12. Chen, T. T., A. Luque, S. Lee, S. M. Anderson, T. Segura, and M. L. Iruela-Arispe. Anchorage of VEGF to the extracellular matrix conveys differential signaling responses to endothelial cells J. Cell Biol. 188:595-609, 2010.

13. Clark, W. A., M. L. Decker, M. Behnke-Barclay, D. M. Janes, and R. S. Decker. Cell contact as an independent factor modulating cardiac myocyte hypertrophy and survival in long-term primary culture J. Mol. Cell. Cardiol. 30:139-155, 1998.

14. Discher, D. E., P. Janmey, and Y. L. Wang. Tissue cells feel and respond to the stiffness of their substrate. Science 310:1139-1143, 2005.

15. Engler, A. J., M. A. Griffin, S. Sen, C. G. Bonnemann, H. L. Sweeney, and D. E. Discher. Myotubes differentiate optimally on substrates with tissue-like stiffness: pathological implications for soft or stiff microenvironments J. Cell Biol. 166:877-887, 2004.

16. Fassler, R., J. Rohwedel, V. Maltsev, W. Bloch, S. Lentini, K. Guan, D. Gullberg, J. Hescheler, K. Addicks, and A. M. Wobus. Differentiation and integrity of cardiac muscle cells are impaired in the absence of beta 1 integrin J. Cell. Sci. 109 (Pt 13):2989-2999, 1996.

17. Feinberg, A. W., A. Feigel, S. S. Shevkoplyas, S. Sheehy, G. M. Whitesides, and K. K. Parker. Muscular thin films for building actuators and powering devices Science 317:1366-1370, 2007.

18. Fink, C., S. Ergun, D. Kralisch, U. Remmers, J. Weil, and T. Eschenhagen. Chronic stretch of engineered heart tissue induces hypertrophy and functional improvement FASEB J. 14:669-679, 2000.

19. Gopalan, S. M., C. Flaim, S. N. Bhatia, M. Hoshijima, R. Knoell, K. R. Chien, J. H. Omens, and A. D. McCulloch. Anisotropic stretch-induced hypertrophy in neonatal ventricular myocytes micropatterned on deformable elastomers. Biotechnol. Bioeng. 81:578-587, 2003.

20. Guan, K., J. Czyz, D. O. Furst, and A. M. Wobus. Expression and cellular distribution of alpha(v)integrins in beta(1)integrin-deficient embryonic stem cell-derived cardiac cells J. Mol. Cell. Cardiol. 33:521-532, 2001.

21. Guo, X. M., Y. S. Zhao, H. X. Chang, C. Y. Wang, L. L. E, X. A. Zhang, C. M. Duan, L. Z. Dong, H. Jiang, J. Li, Y. Song, and X. J. Yang. Creation of engineered cardiac tissue in vitro from mouse embryonic stem cells Circulation 113:2229-2237, 2006.

22. Jacot, J. G., A. D. McCulloch, and J. H. Omens. Substrate stiffness affects the functional maturation of neonatal rat ventricular myocytes Biophys. J. 95:3479-3487, 2008.

23. Kaji, H., Y. Takii, M. Nishizawa, and T. Matsue. Pharmacological characterization of micropatterned cardiac myocytes Biomaterials 24:4239-4244, 2003.

24. Kehat, I., L. Khimovich, O. Caspi, A. Gepstein, R. Shofti, G. Arbel, I. Huber, J. Satin, J. Itskovitz-Eldor, and L. Gepstein. Electromechanical integration of cardiomyocytes derived from human embryonic stem cells Nat. Biotechnol. 22:1282-1289, 2004.

25. Kim, D. H., E. A. Lipke, P. Kim, R. Cheong, S. Thompson, M. Delannoy, K. Y. Suh, L. Tung, and A. Levchenko. Nanoscale cues regulate the structure and function of macroscopic cardiac tissue constructs Proc. Natl. Acad. Sci. U. S. A. 107:565-570, 2010.

26. Kim, J., J. Park, S. Yang, J. Baek, B. Kim, S. H. Lee, E. S. Yoon, K. Chun, and S. Park. Establishment of a fabrication method for a long-term actuated hybrid cell robot Lab. Chip 7:1504-1508, 2007.

27. Kofidis, T., J. L. de Bruin, G. Hoyt, Y. Ho, M. Tanaka, T. Yamane, D. R. Lebl, R. J. Swijnenburg, C. P. Chang, T. Quertermous, and R. C. Robbins. Myocardial restoration with embryonic stem cell bioartificial tissue transplantation J. Heart Lung Transplant. 24:737-744, 2005.

28. Legato, M. J. Sarcomerogenesis in human myocardium J. Mol. Cell. Cardiol. 1:425-437, 1970.

29. Little, C. D. and B. J. Rongish. The extracellular matrix during heart development Experientia 51:873-882, 1995.

30. Liu, J., J. D. Fu, C. W. Siu, and R. A. Li. Functional sarcoplasmic reticulum for calcium handling of human embryonic stem cell-derived cardiomyocytes: insights for driven maturation. Stem Cells 25:3038-3044, 2007.

31. Lunkenheimer, P. P., K. Redmann, N. Kling, X. J. Jiang, K. Rothaus, C. W. Cryer, F. Wubbeling, P. Niederer, P. U. Heitz, S. Y. Ho, and R. H. Anderson. Three-dimensional architecture of the left ventricular myocardium. Anat. Rec. Part A 288A:565-578, 2006.

32. Nussbaum, J., E. Minami, M. A. Laflamme, J. A. Virag, C. B. Ware, A. Masino, V. Muskheli, L. Pabon, H. Reinecke, and C. E. Murry. Transplantation of undifferentiated murine embryonic stem cells in the heart: teratoma formation and immune response FASEB J. 21:1345-1357, 2007.

33. Radisic, M., M. Euloth, L. Yang, R. Langer, L. E. Freed, and G. Vunjak-Novakovic. High-density seeding of myocyte cells for cardiac tissue engineering Biotechnol. Bioeng. 82:403-414, 2003.

34. Radisic, M., H. Park, H. Shing, T. Consi, F. J. Schoen, R. Langer, L. E. Freed, and G. Vunjak-Novakovic. Functional assembly of engineered myocardium by electrical stimulation of cardiac myocytes cultured on scaffolds Proc. Natl. Acad. Sci. U. S. A. 101:18129-18134, 2004.

35. Reppel, M., F. Pillekamp, K. Brockmeier, M. Matzkies, A. Bekcioglu, T. Lipke, F. Nguemo, H. Bonnemeier, and J. Hescheler. The electrocardiogram of human embryonic stem cell-derived cardiomyocytes J. Electrocardiol. 38:166-170, 2005.

36. Ross, R. S. and T. K. Borg. Integrins and the myocardium Circ. Res. 88:1112-1119, 2001.

37. Samuelson, L. C. Differentiation of Embryonic Stem (ES) Cells Using the Hanging Drop Method Cold Spring Harbor Protocols 2006:pdb.prot4485 <last_page> pdb.prot4485, 2006.

38. Sartiani, L., E. Bettiol, F. Stillitano, A. Mugelli, E. Cerbai, and M. E. Jaconi. Developmental changes in cardiomyocytes differentiated from human embryonic stem cells: a molecular and electrophysiological approach. Stem Cells 25:1136-1144, 2007.

39. Seki, S., M. Nagashima, Y. Yamada, M. Tsutsuura, T. Kobayashi, A. Namiki, and N. Tohse. Fetal and postnatal development of Ca2+ transients and Ca2+ sparks in rat cardiomyocytes. Cardiovasc. Res. 58:535-548, 2003.

40. Shapira-Schweitzer, K., M. Habib, L. Gepstein, and D. Seliktar. A photopolymerizable hydrogel for 3-D culture of human embryonic stem cell-derived cardiomyocytes and rat neonatal cardiac cells. J. Mol. Cell. Cardiol. 46:213-224, 2009.

41. Siedner, S., M. Kruger, M. Schroeter, D. Metzler, W. Roell, B. K. Fleischmann, J. Hescheler, G. Pfitzer, and R. Stehle. Developmental changes in contractility and sarcomeric proteins from the early embryonic to the adult stage in the mouse heart J. Physiol. 548:493-505, 2003.

42. Simpson, D. G., L. Terracio, M. Terracio, R. L. Price, D. C. Turner, and T. K. Borg. Modulation of cardiac myocyte phenotype in vitro by the composition and orientation of the extracellular matrix J. Cell. Physiol. 161:89-105, 1994.

43. Snir, M., I. Kehat, A. Gepstein, R. Coleman, J. Itskovitz-Eldor, E. Livne, and L. Gepstein. Assessment of the ultrastructural and proliferative properties of human embryonic stem cell-derived cardiomyocytes Am. J. Physiol. Heart Circ. Physiol. 285:H2355-63, 2003.

44. Soonpaa, M. H., K. K. Kim, L. Pajak, M. Franklin, and L. J. Field. Cardiomyocyte DNA synthesis and binucleation during murine development Am. J. Physiol. 271:H2183-9, 1996.

45. Souren, J. E., C. Schneijdenberg, A. J. Verkleij, and R. Van Wijk. Factors controlling the rhythmic contraction of collagen gels by neonatal heart cells In Vitro Cell. Dev. Biol. 28A:199-204, 1992.

46. Takahashi, T., B. Lord, P. C. Schulze, R. M. Fryer, S. S. Sarang, S. R. Gullans, and R. T. Lee. Ascorbic acid enhances differentiation of embryonic stem cells into cardiac myocytes. Circulation 107:1912-1916, 2003.

47. Tanaka, Y., K. Sato, T. Shimizu, M. Yamato, T. Okano, and T. Kitamori. A micro-spherical heart pump powered by cultured cardiomyocytes Lab. Chip 7:207-212, 2007.

48. van Laake, L. W., R. Passier, J. Monshouwer-Kloots, A. J. Verkleij, D. J. Lips, C. Freund, K. den Ouden, D. Ward-van Oostwaard, J. Korving, L. G. Tertoolen, C. J. van Echteld, P. A. Doevendans, and C. L. Mummery. Human embryonic stem cell-derived cardiomyocytes survive and mature in the mouse heart and transiently improve function after myocardial infarction Stem Cell. Res. 1:9-24, 2007.

49. Vandenburgh, H. H., P. Karlisch, and L. Farr. Maintenance of highly contractile tissue-cultured avian skeletal myotubes in collagen gel In Vitro Cell. Dev. Biol. 24:166-174, 1988.

50. Westfall, M. V., K. A. Pasyk, D. I. Yule, L. C. Samuelson, and J. M. Metzger. Ultrastructure and cell-cell coupling of cardiac myocytes differentiating in embryonic stem cell cultures Cell Motil. Cytoskeleton 36:43-54, 1997.

51. Xi, J., J. J. Schmidt, and C. D. Montemagno. Self-assembled microdevices driven by muscle Nat. Mater. 4:180-184, 2005.

52. Yamamura, N., R. Sudo, M. Ikeda, and K. Tanishita. Effects of the mechanical properties of collagen gel on the in vitro formation of microvessel networks by endothelial cells Tissue Eng. 13:1443-1453, 2007.

53. Yamanaka, S., I. Zahanich, R. P. Wersto, and K. R. Boheler. Enhanced proliferation of monolayer cultures of embryonic stem (ES) cell-derived cardiomyocytes following acute loss of retinoblastoma PLoS One 3:e3896, 2008.

54. Yu, J. G. and B. Russell. Cardiomyocyte remodeling and sarcomere addition after uniaxial static strain in vitro J. Histochem. Cytochem. 53:839-844, 2005.

55. Zak, R. Development and proliferative capacity of cardiac muscle cells Circ. Res. 35:suppl II:17-26, 1974.

56. Zimmermann, W. H., C. Fink, D. Kralisch, U. Remmers, J. Weil, and T. Eschenhagen. Three-dimensional engineered heart tissue from neonatal rat cardiac myocytes Biotechnol. Bioeng. 68:106-114, 2000.

57. Zimmermann, W. H., I. Melnychenko, and T. Eschenhagen. Engineered heart tissue for regeneration of diseased hearts Biomaterials 25:1639-1647, 2004.

Figure Legends

Figure 1: ESCDMs embedded in collagen I hydrogel

ESCDMs are suspended in 2mg/ml collagen I hydrogel immediately after fluorescent sorting. Seeding density was $1.5x10^6$/ml for (a)-(e) and $5x10^6$/ml for (f). These cells are fixed after 21 days. Scale bar for (a)-(f): 100μm; (g): 10μm.

Figure 2: Effect of collagen on cell morphology and elongation on day 2, 7 and 14

(a) Representative images of ESCDMs cultured on gelatin coated polystyrene on day 2, day 7 and day 14. Sarcomeres, visualized with sarcomeric α-actinin, are readily observed as early as 2 days after seeding. Scale bar = 50μm.

(b) Aspect ratio of ESCDMs increases over time regardless of the condition of collagen gel. There is no significant difference in aspect ratio for soluble collagen, compared to control. There is a slight decrease in aspect ratio for the collagen gel condition compared to control after 14 days. Asterisks represent statistical difference ($p<0.05$) of the data point of interest compared to day 2 of the same condition and diamond (◊) stands for statistical difference ($p<0.05$) of the data point of interest compared to the control condition without additional collagen I of the same day.

(c) There is a difference in the rate of aspect ratio increase for different collagen conditions. ESCDMs cultured with soluble collagen elongate most rapidly, followed by control and collagen gel.

Figure 3: Percentage of binucleated cells with various collagen I condition

Effect of collagen I on binucleation is presented. (a) ESCDMs are either exposed to no collagen, soluble collagen (50μg/ml) or 2mg/ml collagen gel laden on top of the monolayer seeded on an isotropic surface. Binucleation increases over time. Soluble collagen, supplemented in the medium, has a strong negative effect for binucleation. (b) Number of cells for different collagen conditions. Asterisks represent

statistical difference ($p<0.05$) of the data point of interest compared to day 2 of the same condition and diamond (◊) stands for statistical difference ($p<0.05$) of the data point of interest compared to the control condition without additional collagen I of the same day.

Figure 4: cell alignment with microcontact printing and nanopattern topography

(a) Two methods of patterning were tested – microcontact printing (MCP) and nanopattern topography (NPT). MCP was visualized by printing gelatin conjugated with Oregon green.

(b&c) Cells exhibit clear alignment when cultured on MCP and NPT surfaces. These are representative images of nuclei (DAPI), sarcomeric α-actinin and merged cells from day 14 samples with 50µg/ml soluble collagen.Scale bars: (b) 50µm, (c) 10µm.

Figure 5: histograms of cell alignment at different time points

Histograms of cell alignment at (a) day 2, (b) day 7, and (c) day 14 are plotted. Three surface patterns are compared: no patterns, MCP, and NPT. Three extracellular matrix incorporations are compared for day 7 and day 14 (the conditions do not apply to day 2 samples because they are applied on day 3): no additional ECM, 50µg/ml soluble collagen I in media and 2mg/ml collagen hydrogel laden on the surface of the monolayer. Because of the secretion of ECM by the cells, we tested if the alignment would be maintained on MCP surface at day 14. (d) illustrates that while ESDMs cultured without collagen and with soluble collagen lose alignment, alignment for ESCDM monolayers laden with collagen gel is rescued.

Figure 6: Effect of surface patterning on elongation without the addition of collagen

Effect of surface patterning on cell elongation is measured. (a,b) Aspect ratio of cells on isotropic and NPT surfaces increases over time while that of cells on MCP surface remains constant. (c,d) The average dimensions of the major and minor axes are also recorded and it can be seen that most increase in aspect ratio is attributed to a decrease in minor axis. Asterisks represent statistical difference ($p<0.05$) of the data

point of interest compared to day 2 of the same condition and diamond (◊) stands for statistical difference ($p<0.05$) of the data point of interest compared to the isotropic condition of the same day.

Figure 7: Effect of surface patterning on binucleation

(a) Binucleation with surface patterning. MCP accelerates binucleation between day 2 and day 7. (b) NPT is a negative regulator of binucleation. (c) By examining the number of cells, there are a higher number of cells on NPT surface after 14 days suggesting that the decrease in binucleation is a result of an increase in cytokinesis. Asterisks represent statistical difference ($p<0.05$) of the data point of interest compared to day 2 of the same condition and diamond (◊) stands for statistical difference ($p<0.05$) of the data point of interest compared to the isotropic condition of the same day.

Figure 1
Click here to download high resolution image

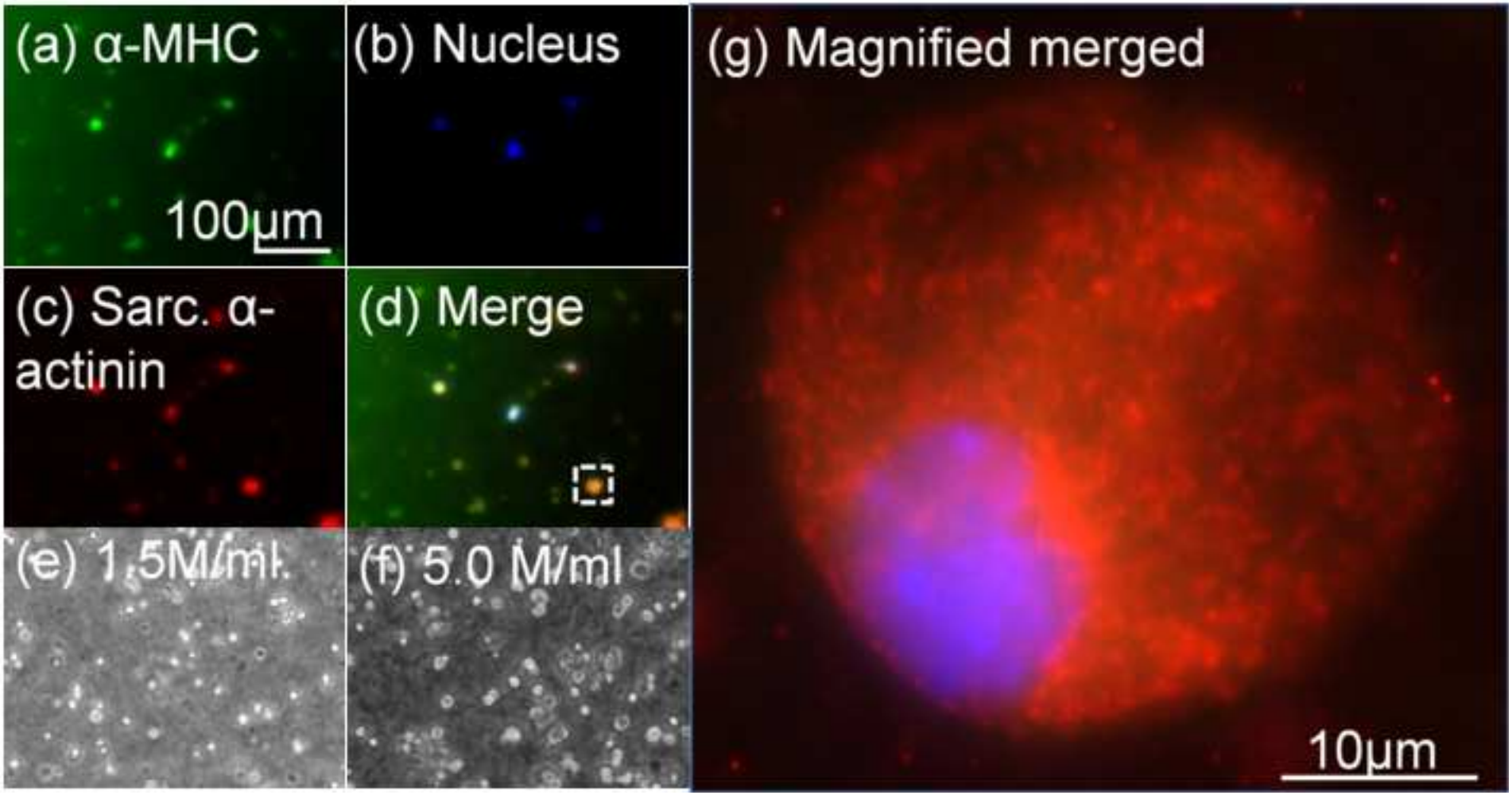

Figure 2

Click here to download high resolution image

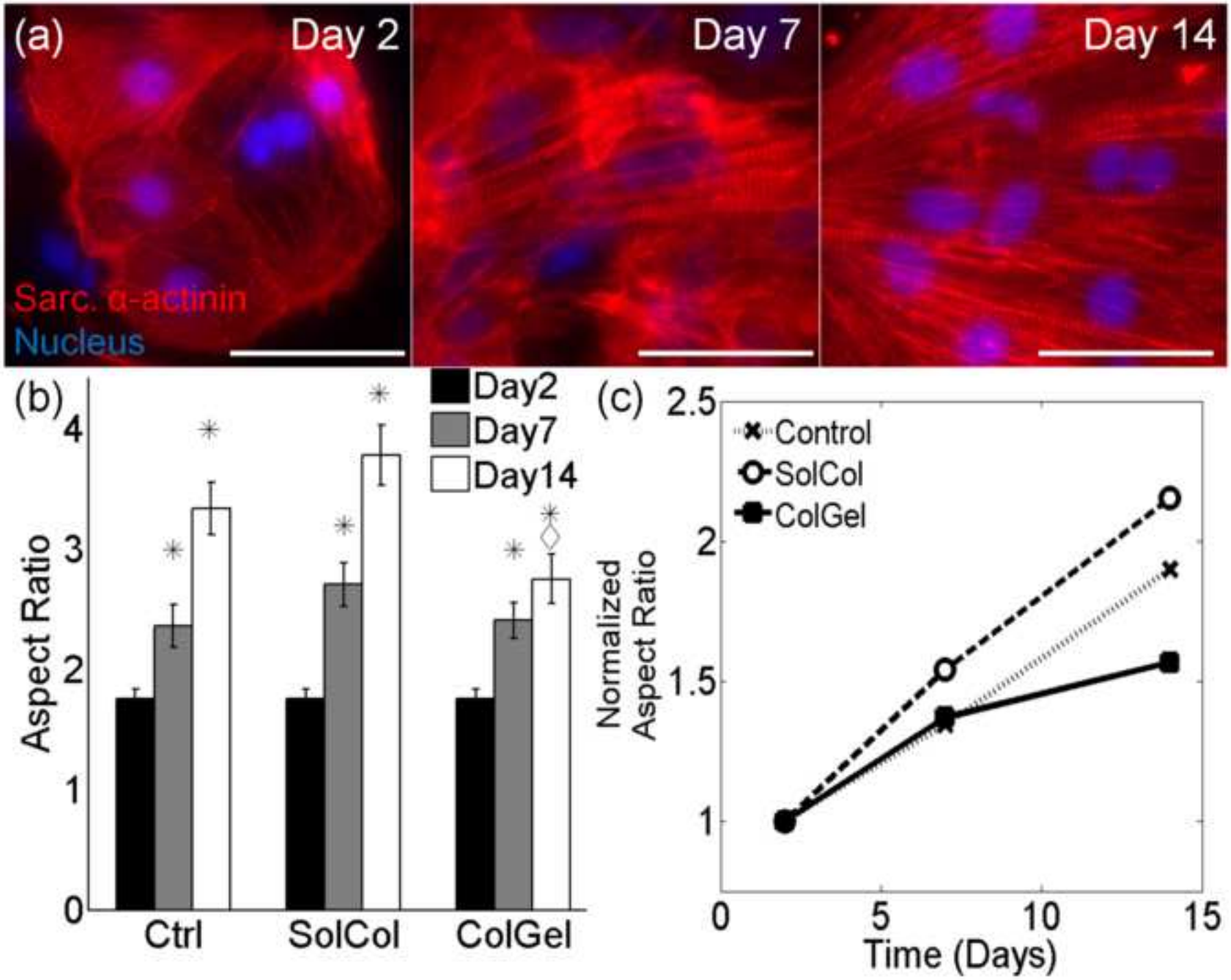

Figure 3
Click here to download Figure: figure3.eps

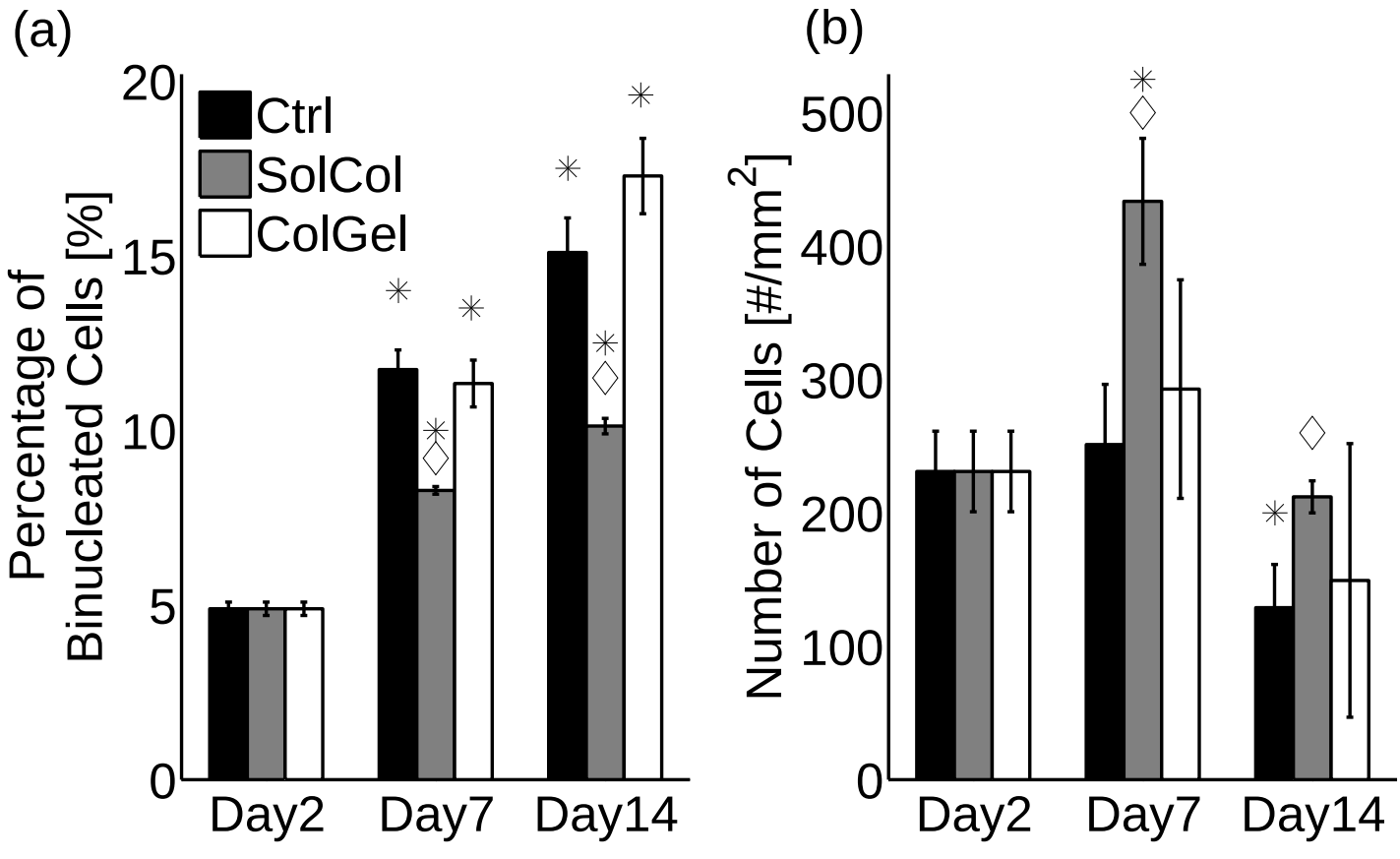

Figure 4
Click here to download high resolution image

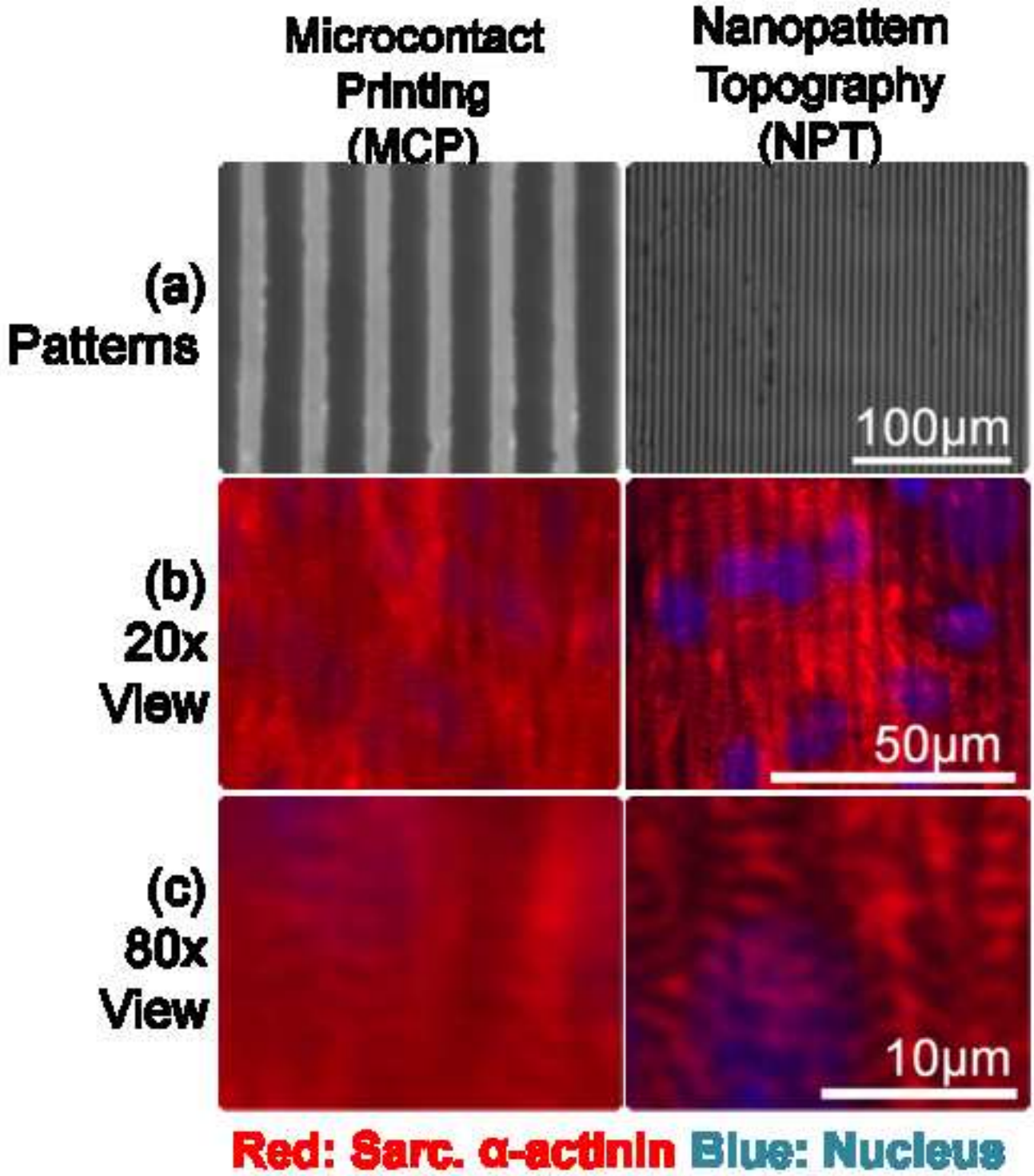

Figure 5

Click here to download Figure: figure5.eps

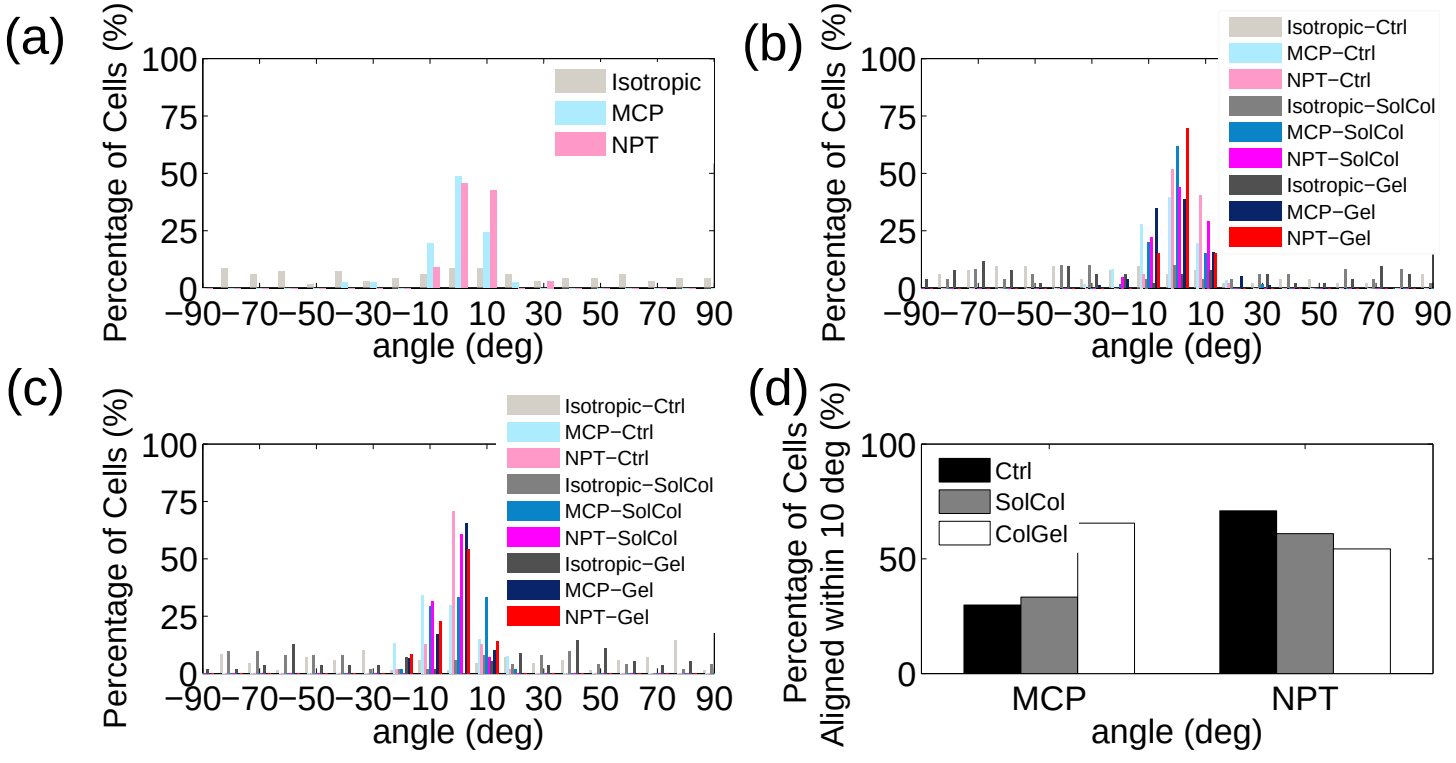

Figure 6
Click here to download Figure: figure6.eps

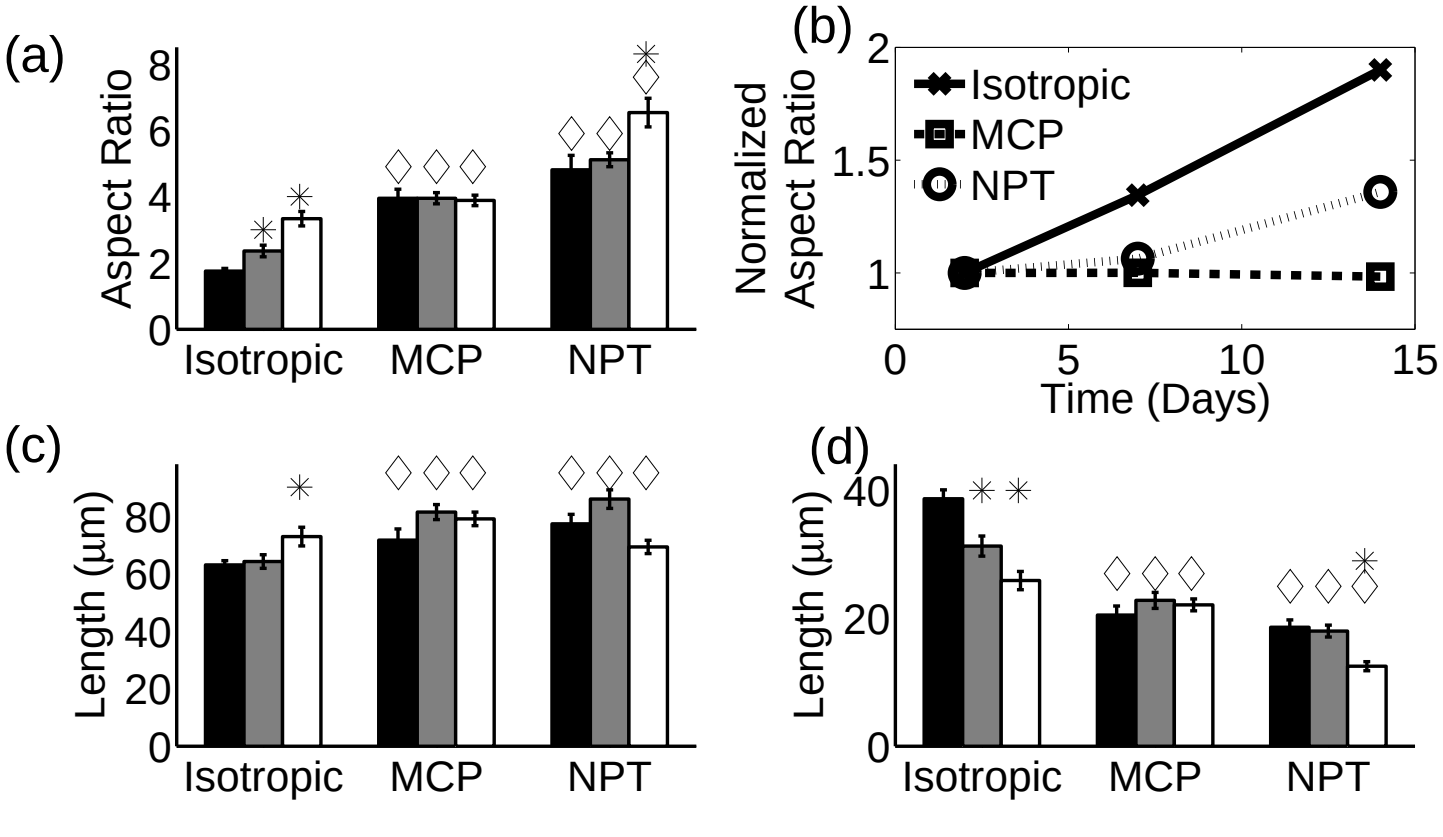

Figure 7

Click here to download Figure: figure7.eps